CO_2 adsorbent pellets produced from pine sawdust: effect of coal tar pitch addition

M.G. Plaza, I. Durán, F. Rubiera, C. Pevida*

Instituto Nacional del Carbón, INCAR-CSIC, Apartado 73, 33080, Oviedo, Spain

Abstract

The main drawbacks of developing carbon adsorbents from pine sawdust, an abundant biomass feedstock, are the low carbon yield of the process and the poor mechanical properties of the resulting carbons. In an attempt to overcome these limitations, the effect of the addition of coal tar pitch was assessed. Adsorbent pellets were produced from pine sawdust and coal tar pitch by activation with CO_2. The preparation process was optimized by using as decision variables the carbon yield and the adsorption performance of the adsorbents in conditions representative of post-combustion capture applications (10% CO_2 at atmospheric pressure and at 50 °C). Subjecting the composite pellets to a pre-oxidation treatment with air increased the carbon yield of the production process, and also improved the adsorption kinetics and capacity of the final adsorbents. The prepared adsorbents present a high carbon yield, a superior mechanical resistance and a competitive adsorption performance.

Keywords: biomass, adsorbents, carbon, CO_2 capture

1. Introduction

Biomass is a renewable and globally distributed source of carbon that needs to be exploited in a sustainable way. The processing of biomass to obtain activated carbons has been known since ancient times. In fact, many commercial activated carbons are produced from biomass sources, such as wood or coconut shells. The process generally consists in subjecting the biomass to a carbonization process to reduce its volatile content and thereby increase its carbon content, followed by an activation stage where CO_2, H_2O or air react with the carbon and develop its inner pore structure. This process is commonly referred to as "*physical activation*" in opposition to "*chemical activation*", where the gaseous activating agents are replaced by KOH, $ZnCl_2$, H_2SO_4, H_3PO_4, *etc*. Further details about the preparation of carbon adsorbents from different biomass resources can be found elsewhere [1, 2].

*corresponding author email: *cpevida@incar.csic.es* (C. Pevida)

Carbon adsorbents developed from different agricultural and food industry residues have shown potential as adsorbents for CO_2 capture applications [3-13]. These materials present the added advantage that they have fixed atmospheric carbon during their growth, reducing the carbon footprint of the final material. Carbon capture technologies will need to play a key role in the transition to an alternative energy scenario that is not dependent on fossil fuels. The reduction of the emissions of existing large stationary sources like power plants and cement plants is challenging due to the low partial pressure of CO_2 in the stack gases. Amine scrubbing, used for the removal of CO_2 from natural gas, could be a suitable technology for carrying out this separation process in existing power plants. However, this is an energy intensive process due to the need to heat a vast amount of water (near 70 wt.%) in order to regenerate the solvent: steam consumption accounts for over half of the operating costs of the capture unit [14]. Installing CCS into the power supply system would cause a decrease in power output of about 10%, two thirds of which is due to the capture step. Adsorption separation processes seek to reduce the energy penalty of the capture step compared to the amine scrubbing alternative [16-18]. By means of this technology, CO_2 would be removed from the flue gas by the preferential adsorption of CO_2 over the other flue gas components, like N_2, which is the major component of flue gas. In order to work in a continuous operation mode, the adsorbent needs to be regenerated. This can be achieved by reducing the partial pressure of CO_2 in the vessel that holds the adsorbent (usually by means of vacuum, which is commonly referred to as vacuum swing adsorption, VSA), or by increasing the adsorbent temperature (which is called temperature swing adsorption, TSA), or by a combination of both (VTSA). The design of the adsorption process will be intrinsically related to the properties of the adsorbent. The ideal adsorbent must be available, of low cost, high resistance, show sufficient adsorption capacity and selectivity under the operation conditions, and be easily regenerated. Moreover, for the adsorbents to be used in fixed-bed gas separation processes operating in VSA and TSA modes the sorbent particles must be first moulded into macroscopic shapes, since fine powder cannot be used directly due to pressure drop constraints [19].

In this work carbon adsorbents have been developed from pine sawdust. The use of sawdust as feedstock is gaining increasing attention due to the decreasing availability of wood resources. Moreover, the cost of wood can represent as much as 50% of the cost of producing charcoal in a conventional kiln [20], so that there is a strong economic incentive for replacing wood by a wood byproduct of lower commercial value. The use of wood-based activated carbons is customary in liquid phase adsorption applications. However, there are fewer studies on gas phase adsorption using wood-based activated carbons. Pietrzak *et al.* have evaluated

activated carbons obtained from pine sawdust as adsorbents for NO_2 removal [21, 22]. KOH activated paulownia sawdust [11] and H_3PO_4 activated eucaliptus wood [23] have recently been proposed for CO_2 adsorption. In the present work, carbon adsorbents are developed from pine sawdust through single-step activation with CO_2, which has less environmental impact than the chemical route. However, the main drawback of the physical route is a lower carbon yield [24]. Sawdust-derived carbons present lower carbon yield and weaker mechanical resistance compared to other adsorbents. Organic binders are commonly used to obtain granular activated carbons from agricultural residues [25, 26]. Coal tar pitch has been used as binding material in carbon monoliths with superior mechanical properties [27]. Therefore, in order to improve the carbon yield and the mechanical properties of the pine sawdust derived carbons, composite pellets containing pine sawdust and coal tar pitch were produced. The effect of coal tar pitch addition on the physical properties of the adsorbent pellets, on their carbon yield, and on their adsorptive properties was assessed. The composite carbons not only presented a superior mechanical resistance, but also an extraordinarily high carbon yield, which would have a great impact on the economic cost of the production process [24]. Moreover, by subjecting the composite pellets to an air oxidation pretreatment prior to their activation with carbon dioxide, the carbon yield of the adsorbents can be further increased, and their CO_2 adsorption performance enhanced not only in terms of adsorption capacity but also in terms of the adsorption and desorption rate. The production process could be easily implemented in industry given that extrusion, oxidation and activation are common practice in activated carbon production plants [26, 28].

2. Materials and methods

2.1. Materials

Pine woodchips were reduced to a particle size below 1 mm (pine sawdust, PS) before being subjected to further processing. A high temperature binding coal tar pitch (CT) in pencil shape with a softening point of 110 °C was ground and sieved and a particle size fraction of between 150 and 212 µm was selected for the present study. The pine sawdust (PS) and the coal tar pitch (CT) were blended in PS to CT mass ratios of 10:1, 10:2 and 10:5, and thoroughly mixed to ensure homogeneity. The resulting blends and the pine sawdust alone were then conformed into cylindrical pellets 4 mm in diameter by uniaxial compression in a stamping tablet machine. The pelletized samples will be referred to as PPSCT101, PPSCT102, PPSCT105 and PPS. The pellet density was easily calculated due to its regular cylindrical shape by dividing the mass of a single pellet by its volume.

2.2. Optimization of activation conditions in a thermogravimetric analyzer

The pellets of the PS and PS-CT blends were activated with CO_2 in a single step procedure. To evaluate the effect of the activation parameters (*i.e.*: activation temperature and time), a series of activation tests was carried out in a thermogravimetric analyzer, by applying a total flow rate of 100 cm^3 min^{-1} of an equimolar mixture of CO_2 and N_2, a heating rate of 5 °C min^{-1} up to the set point activation temperature and a pre-determined soaking time. The samples were dried *in situ* at 100 °C for 1 h prior to the activation tests. The yield of the activation process was calculated as follows:

$$CY_{Activation}(\%) = \frac{m_{fA}}{m_0} \times 100 \quad (1)$$

where m_{fA} represents the final mass of the sample at the end of the activation procedure, and m_0 the mass of the sample at the end of the drying step.

Oxidation treatments are commonly used in industry to reduce the swelling of coal tar pitch during the carbonization of composite materials. It is also known that oxidation treatment with air at moderate temperatures increases the carbon yield of the coal tar pitch due to the polymerization of light components to form cross-linked molecules [29]. To evaluate the effect of air oxidation pretreatment of the composite pellets on the properties of the final carbons, a series of oxidation tests was carried out in the thermogravimetric analyzer. The tests consisted in heating the pellets in 50 cm^3 min^{-1} of air at a heating rate of 5 °C min^{-1} up to the desired oxidation temperature, and holding this temperature for a given time. First, the effect of oxidation time was evaluated for a fixed oxidation temperature of 275 °C. This temperature was selected as a starting point based on a previous study that dealt with the effect of air-blown treatments on a coal tar pitch [29]. Several oxidation times were evaluated: 1, 2, 4 and 6 h. On the basis of these results, an optimal oxidation time was selected and the effect of the oxidation temperature was assessed.

The carbon yield of the oxidation treatment was calculated as follows:

$$CY_{oxidation}(\%) = \left(\frac{m_{fox}}{m_0}\right) \times 100 \quad (2)$$

where m_{fox} is the final mass of sample remaining at the end of the oxidation treatment, and m_0 the mass of the dry green pellet.

The oxidized pellets were subsequently activated following the same procedure as described before. An overall carbon yield (mass of the final adsorbent obtained per mass of the dry green

pellets) was calculated from the yields of the oxidation and activation steps to compare the results with the non-oxidized activated pellets:

$$Overall\ yield\ (\%) = \left(\frac{CY_{oxidation}}{100} \times \frac{CY_{activation}}{100}\right) \times 100 = \left(\frac{m_{fA}}{m_o}\right) \times 100 \quad (3)$$

2.2. Sample screening: gravimetric adsorption tests

The adsorption behaviour of the activated pellets in conditions representative of post-combustion capture (50 °C and low partial pressure of CO_2) was evaluated at atmospheric pressure in a thermogravimetric analyzer. The results of the evaluated adsorbents were compared to those of a reference commercial activated carbon, Norit R2030CO2, used for CO_2 removal in cold wharehouses.

After an initial conditioning step, carried out in 100 $cm^3\ min^{-1}$ of N_2 at 100 °C for 1 h, the samples were cooled down to the adsorption temperature in the N_2 flow. The mass of the samples increases during the cooling stage due to the adsorption of N_2. Once the temperature of the sample stabilises, so does the mass of the sample (the sample reaches thermal and adsorption equilibrium with the surrounding atmosphere). Buoyancy and dragging effects were appropriately corrected by running blank experiments. Assuming that the adsorption capacity of N_2 at 100 °C can be considered negligible, it is possible to estimate the adsorption capacity of pure N_2 (q_{N_2}) at the adsorption temperature (50 °C) as follows:

$$q_{N_2}(wt.\%) = \frac{m_{50,\,N_2} - m_{100,\,N_2}}{m_{100,\,N_2}} \times 100 \quad (4)$$

where $m_{100,\,N_2}$ is the mass of the sample measured at the end of the drying step at 100 °C in the N_2 flow, and $m_{50,\,N_2}$ is the the mass of sample at 50 °C at the end of the cooling step in the N_2 flow.

After 1 h, the composition of the feed was switched from 100 % N_2 to a mixture consisting of 10% CO_2 and 90% N_2 and the temperature was kept constant. As a consequence, the mass of the sample increased due to the adsorption of CO_2 from the gas mixture. The total mass uptake is expressed as weight percentage taking as reference the mass of the sample at the end of the drying step (as mentioned before, the adsorption capacity of N_2 at 100 °C is assumed to be negligible):

$$q_{N_2+CO_2}\ (wt.\%) = \frac{m_{50,(N_2+\,CO_2)} - m_{100,\,N_2}}{m_{100,\,N_2}} \times 100 \quad (5)$$

where $q_{N_2+CO_2}$ is the total mass uptake, which includes the amount of CO_2 and N_2 adsorbed and $m_{50,(N_2+\,CO_2)}$ is the mass of the sample in the flow of the 10% CO_2-90% N_2 mixture at the end of the adsorption step at 50 °C. Finally, the samples were regenerated by switching the composition of the gas back to 100% N_2 at constant temperature.

If mass transfer resistances are negligible, the equilibrium of adsorption will be attained immediately. However, this is rarely the case. The rate of adsorption is frequently represented by simple models that lump together the mass transfer resistances that can retard the adsorption process (*i.e.:* external diffusion in the film surrounding the particle, diffusion into the pore system, and surface diffusion) in a single overall mass transfer coefficient. The one most commonly used is the solid film linear driving force approximation (LDF) which is a pseudo-first order model that considers that the adsorption rate is proportional to the number of free adsorption sites:

$$\frac{dq}{dt} = k(q_e - q) \tag{6}$$

where k is the apparent adsorption rate constant, q_e represents the amount adsorbed at equilibrium, and q the amount adsorbed at a given time. By integrating Equation 6 with the following boundary conditions: for *t=0 q=0* and for *t=∞ q=*q_e, we obtain the following expression for the uptake curve [30]:

$$q = q_e\left(1 - e^{-kt}\right) \tag{7}$$

Another form of the lumped model is the quadratic driving force (QDF) approximation, which is a pseudo-second order model that allows a greater dependence on loading than the LDF model. This model is useful for describing solid diffusion rate controlled processes that are not properly described by the LDF approximation.

$$\frac{dq}{dt} = k(q_e - q)^2 \tag{8}$$

The corresponding integrated equation with the aforementioned boundary conditions is:

$$q = \frac{{q_e}^2 kt}{1 + q_e kt} \tag{9}$$

The apparent rate constants of the lumped models were fitted to minimize the sum of square residuals between the experimental mass uptake and that given by the model:

$$Goodness\ of\ fit = \sqrt{\frac{\sum_{i=1}^{N}\left(\mathrm{q}_{exp} - \mathrm{q}_{model}\right)_i^2}{N-1}} \times 100 \quad (10)$$

where *N* represents the number of experimental data points fitted for each sample (from the beginning of the mass uptake up to the equilibrium $\left({}^{q}/_{q_e} = 1\right)$).

2.3. Adsorbent preparation and characterization

After the sample screening stage, a greater amount of adsorbent was prepared in a vertical furnace using a double jacketed fixed-bed quartz reactor in the conditions identified as optimal. The inner reactor (I.D. 2 cm) has a porous plate in its base that holds the sample (4-5 g). Gases are fed from the upper end of the jacket, so that they are preheated before contacting the sample bed. The flow rate and composition of the feed gas is controlled by mass flow controllers. A total flow rate of 100 $cm^3\ min^{-1}$ was used during the oxidation and activation treatments. The tars that exit the reactor were condensed by means of an ice bath and weighed at the end of the experiment. The gas yield was calculated by difference.

The porous texture of the adsorbents was characterized by physical adsorption of N_2 at -196 °C in an automated volumetric apparatus. The total pore volume was obtained from the amount of N_2 adsorbed at a relative pressure of 0.99. The micropore volume was determined by the Dubinin-Radushkevich method (DR) and the average micropore width was estimated from the Stoeckli-Ballerini relation [31].

The morphology of the adsorbents was assessed by Field Emission Scanning Electron Microscopy (FESEM) in a Quanta FEG 650.

The mechanical strength and attrition resistance of the adsorbent pellets was evaluated subjecting 10 pellets to 3000 revolutions at 35 rpm in a rotary drum equipped with two inner lifters (see [32] for further details). The hardness number of an activated carbon is usually measured as the change in weight, expressed as a percentage of a specific screen size fraction after the sample has been subjected to a mechanical test method (vibration, impact, rotary motion, or motion) [33, 34]. Herein it was calculated as the change in weight, expressed as a percentage of the size fraction above 1 mm, after the aforementioned rotary test.

3. Results and discussion

3.1. Raw materials

The ultimate and proximate analysis results of the raw materials used in the present study, pine sawdust (PS) and coal tar pitch (CT), can be found in Table 1.

Table 1. Ultimate and proximate analyses of the raw materials: pine sawdust (PS) and coal tar pitch (CT)

Sample	Ultimate analysis				Proximate analysis (wt. %, daf)				
	Moisture (%)	Ash (%, db)	VM (%, db)	FC* (%, db)	C	H	N	S	O*
PS	9.2	0.6	84.6	14.8	51.1	6.2	0.3	0.0	42.4
CT	0.1	0.0	45.3	54.7	94.1	4.1	1.0	0.5	0.3

*Calculated by difference; VM: Volatile matter; FC: Fixed carbon; db: dry basis; daf: dry ash free basis

The ash content of the raw materials is nearly negligible, which is highly desirable for the development of carbon materials.

The high volatile matter content of PS is the reason for the low carbon yield associated to carbons developed from this renewable source. The total carbon yield of wood-based physical activated carbons is of the order of 12.5 wt% [24]. Given that the volatile matter content of the coal tar pitch is approximately half that of the pine sawdust, the addition of coal tar pitch can be expected to increase the carbon yield of the composite materials.

The most abundant element of pine sawdust is carbon, followed by oxygen, and by hydrogen to a much lesser amount, as expected for a typical pine wood composition: approximately 42% cellulose, 25 % hemicellulose, and 30 % lignin. The principal component, cellulose, is a macropolymer of glucose (about 10 000 units) which forms tiny microfibers that aggregate to form larger fibers; hemicellulose is a smaller polymer of glucose (150 - 200 units) that fills the spaces between the cellulose fibers; and lignin is a phenolic compound that is tightly bound to cellulose. On the other hand, coal tar pitch is mainly composed of carbon (94 %), with minor contributions from hydrogen, nitrogen, sulfur, and oxygen. Coal tar pitch is the heavy product obtained from the high-temperature distillation of coal tar. It is composed of a complex mixture of three or more condensed aromatic ring hydrocarbons. The C/H atomic ratio, usually taken as a measure of aromaticity, has a value of 1.9 for the coal tar pitch and of 0.7 for the pine sawdust.

3.2. Pelletization of the pine sawdust and the blends of pine sawdust and coal tar pitch

The diameter of the green pellets is given by the punch and die set installed in the press unit. The height of the pellet depends on the amount loaded, the physical properties of the material

to be pelletized and the pressure applied. Table 2 shows the average dimensions and the pellet density measured for a number *N* of green pellets with different compositions (the standard deviation is shown in parentheses). As can be seen from the table, the density of the green pellets is approximately 1.1 g cm^{-3}, with little influence from their composition.

Table 2. Dimensions and density of the green pellets of pine sawdust (PS) and blends of pine sawdust and coal tar pitch (CT).

PS:CT mass ratio	Pellet diameter (mm)	Pellet height (mm)	Pellet density (g cm^{-3})	N
10:0	4.1 (± 0.0)	3.4 (± 0.1)	1.193 (±0.022)	8
10:1	4.1 (± 0.0)	3.1 (± 0.1)	1.139 (± 0.019)	15
10:2	4.1 (± 0.0)	3.2 (± 0.1)	1.112 (±0.019)	15
10:5	4.1 (± 0.0)	3.5 (± 0.2)	1.162 (±0.018)	25

3.3. Effect of activation temperature

Prior to activating the pellets, the thermal behavior and reactivity of the green materials towards CO_2 was assessed in a thermogravimetric analyzer by subjecting them to a heating rate of 5 °C min^{-1} up to 900 °C using a total flow rate of 100 cm^3 min^{-1} of an equimolar mixture of CO_2 and N_2 (these results can be found in the supporting information). PPS shows the typical thermal degradation of lignocellulosic materials, with contributions from the decomposition of the hemicellulose, cellulose and lignin fractions, where the temperature interval of the degradation of the individual constituents partly overlaps each other. The devolatilization of PPS starts at about 200 °C, and most of the volatile material decomposes below 400 °C, with the maximum rate of mass loss occurring at 360 °C. The rate of mass loss starts to increase again above 700 °C due to the partial gasification of the remaining char by CO_2:

$$C_{char} + CO_{2\,(g)} \rightarrow 2CO_{(g)} \quad \Delta H = 172.67 \frac{kJ}{mol} \tag{11}$$

The thermal decomposition of the coal tar pitch (CT) takes place in a similar temperature range to that of PPS, between 200 °C and 600 °C. However, the maximum devolatilization rate is shifted to higher temperatures: 406 °C. The rate of mass loss between 591 °C and 842 °C is negligible (< 0.001 % s^{-1}). However, above this temperature and up to 900 °C there is a slight increase in the rate of mass loss (≈ 0.001 % s^{-1}) that can be attributed to the gasification of coal tar pitch by CO_2. The composite pellets (PPSCT) present an intermediate behavior between PPS and CT. The thermal decomposition profile is similar to that of PPS, although the rate of mass

loss is lower. The reactivity of PPSCT105 towards CO_2 at high temperatures is also intermediate between those of PPS and CT.

To evaluate the effect of the temperature of activation, the pellets of pine sawdust (PPS) and the pellets of the pine sawdust and coal tar pitch blends (PPSCT series) were heated at 5 °C min^{-1} up to three different temperatures, 700, 800 and 900 °C and held at these temperatures for 30 min in 100 cm^3 min^{-1} of an equimolar mixture of CO_2 and N_2 in a thermogravimetric analyzer. The activated pellets were identified by the precursor name followed by letter A (activation) and the temperature of activation (for example, the activated pellets of pine sawdust will be referred to as PPSA7, PPSA8 and PPSA9). The coal tar pitch with a particle size between 150 and 212 μm (CT) was subjected to the same activation protocol for comparison purposes. Figure 1 shows the activation yields of all these samples. As expected, the yield decreases with increasing temperature due to the increase in the gasification rate with CO_2. On the other hand, the carbon yield increases with the coal tar pitch content in the blend due to the lower volatile content of CT and its lesser reactivity towards CO_2. In general, the yield from the activation of the pellets made from the pine sawdust and coal tar pitch blends is higher than might be expected from their composition according to the additive rule (represented by the dashed lines in Figure 1). Moreover, this difference becomes more apparent when the content of coal tar pitch in the blend is increased (up to 30% above the expected yield for the PS:CT mass ratio of 10:5). The higher yield observed for the pellets made from blends of pine sawdust and coal tar pitch is probably related to interactions between these two components during the heating process. Similar interactions have been identified during the carbonization of sawdust and petroleum pitch composites [35]. The production cost of activated carbons is very sensitive to the product yield [24]: a higher total carbon yield means a lower installation and operational costs primarily due to the need to treat a smaller amount of feedstock to reach a given level of production. Therefore there is a strong economic incentive to improve the carbon yield of the wood-based activated carbon production process.

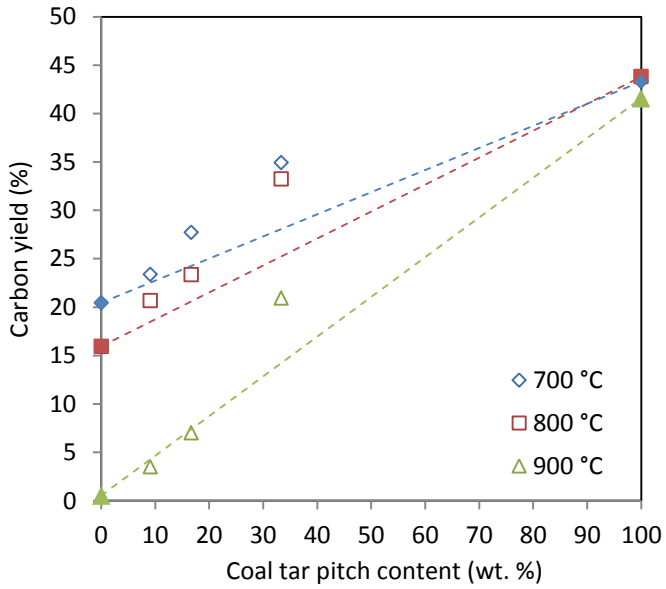

Figure 1. Influence of activation temperature and blend composition on the carbon yield of PPS, CT and PPSCT series activated with CO_2 at 700, 800 and 900 °C for 30 min in a thermogravimetric analyzer. Dashed lines represent the expected yield according to the additive rule.

Except for the highest temperature evaluated, 900 °C, and only for the two samples with the highest pine content, PPSA9 and PPSCT101A9, the pellets maintained their cylindrical shape after activation. The mass loss occurring during activation was accompanied by a reduction in the outer volume of the pellet of at least 50 %. Table 3 shows the density of the activated pellets, which is lower than that of the green pellets (see Table 2) due to the creation of internal porosity by the loss of volatile matter during heating and by the gasification of the remaining char with CO_2. For a given composition, the pellet density decreases sharply at 900 °C due to a substantial increase in the gasification rate of pine sawdust with CO_2. For a given activation temperature, the pellet density increases with the coal tar pitch content, because of its smaller volatiles content and its lower reactivity towards CO_2. It must be borne in mind that a high density is desirable, as it determines (together with the adsorption capacity, which is generally expressed on a mass basis) the volume of the adsorbent required for a determined application. Moreover, during handling, it was observed that the mechanical resistance of the composite pellets was superior to that of the pellets made from the pine sawdust alone.

Table 3. Density of the pellets of pine sawdust (PS) and blends of pine sawdust and coal tar pitch (CT) activated with CO_2 at different temperatures.

PS:CT	Pellet density (g cm^{-3})		
mass ratio	Activation at 700 °C	Activation at 800 °C	Activation at 900 °C
10:0	0.513	0.445	-
10:1	0.546	0.553	-
10:2	0.587	0.652	0.241
10:5	0.796	0.795	0.544

Figure 2a shows the adsorption capacity of the activated pellets of pine sawdust and blends of pine sawdust and coal tar pitch in a mixture consisting of 10% CO_2 (balance N_2) at atmospheric pressure and at 50 °C, expressed on a mass basis. A commercial activated carbon, Norit R2030 CO2, used for the removal of CO_2 in cold warehouses, has been included for comparison purposes. In general, the adsorption capacity decreases with the coal tar pitch content and increases with the temperature of the activation for a given composition. However, the gasification of pine sawdust at 900 °C was so severe that it was not possible to recover samples PPSA9 and PPSCT101A9 for the adsorption test (the pellets disintegrated during activation).

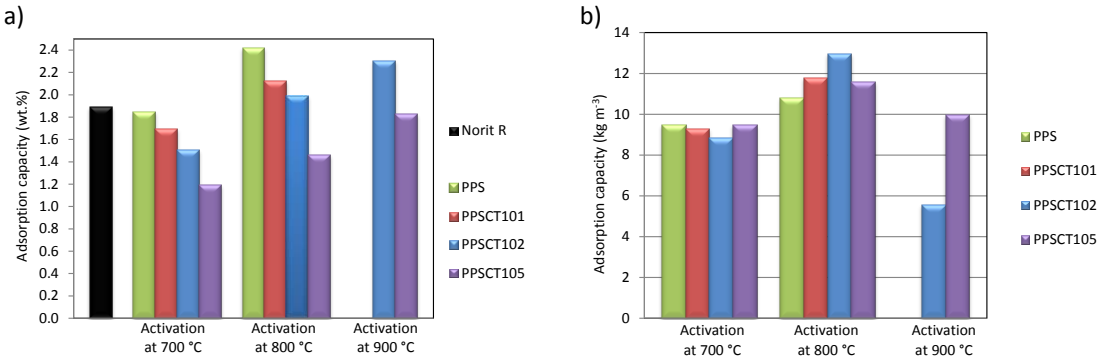

Figure 2. Equilibrium adsorption capacity at 50 °C and at atmospheric pressure in a mixture consisting of 10% CO_2 (balance N_2), expressed on: (a) a mass basis and (b) a volumetric basis (calculated using the pellet density).

The maximum adsorption capacity on a mass basis, Figure 2a, was attained by the pine sawdust pellet activated at 800 °C, which is even superior to that of the reference carbon. However, the carbon yield of PPSA8 was half of that of PPSCT105A8 (16 *vs.* 33%). By increasing the activation time of PPS up to 60 min at 800 °C, it was possible to increase the adsorption capacity up to 2.8 wt.% at the expense of reducing the carbon yield down to 12% (which is a typical yield for physically activated wood-based carbons [24]).

PPSCT102A9 is the sample with the second highest adsorption capacity after PPSA8. Nonetheless, the carbon yield of this sample is only 7%. On the other hand, PPSCT105A9 shows an adsorption capacity close to that of the reference carbon and a significantly higher carbon yield of nearly 21%.

If the adsorption capacity of the samples is compared on a volumetric basis (Figure 2b), by means of the pellet densities shown in Table 3, the samples prepared from the blends of coal tar pitch and pine sawdust by activation at 800 °C become those with the greatest capacity.

Figure 3a shows the results of the full adsorption experiments for the series activated at 700 °C in terms of total mass uptake *versus* time. Note that the samples are regenerated by simply switching the feed gas back to 100% N_2 at constant temperature. All the samples present fast adsorption and desorption kinetics, except that with the highest coal tar pitch content, PPSCT105A7. Similar results were obtained for the series activated at 800 °C.

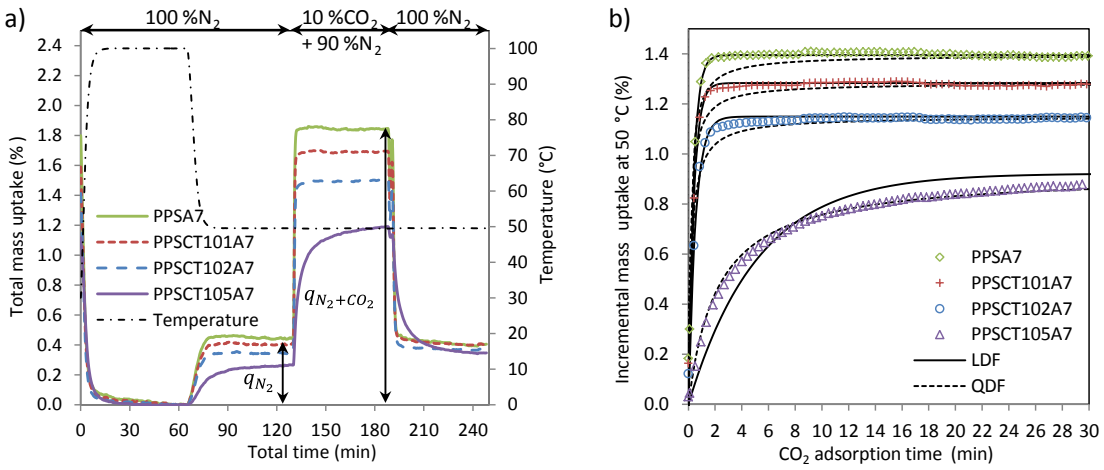

Figure 3. Effect of the coal tar pitch content on the adsorption performance of the pellets activated at 700 °C: (a) total mass uptake *versus* time (full experiment); (b) incremental mass uptake when the composition of the feed gas is changed from 100% N_2 to a mixture consisting of 90% N_2 and 10% CO_2 at 50 °C.

Fast adsorption and desorption kinetics are mandatory for the use of the adsorbents in a post-combustion CO_2 capture process, due to the large flow rates involved (rapid swing cycles are required to maximize the throughput). To evaluate the kinetics of adsorption, the dynamic mass uptake of the samples from the gas mixture was represented taking as a reference the mass of sample at the end of the conditioning step in N_2 at 50 °C (see Figure 3b). This incremental mass uptake corresponds to the adsorption of CO_2 from the mixture. However, the amount of CO_2 adsorbed at equilibrium is expected to be somewhat higher than this incremental uptake, due to the displacement of part of the N_2 initially adsorbed (the partial pressure of N_2 decreases, and CO_2 is expected to be preferentially adsorbed over N_2 due to its

higher quadrupole moment). As shown in Figure 3b, the adsorption rate from the mixture can be approximately represented by the lumped models described in section 2. The LDF approximation suitably describes the mass uptake of the pellets with a higher pine content, but fails to describe the slower approach to equilibrium of PPSCT105A7. The latter is better represented by the pseudo-second order model, which shows a stronger dependence of the adsorption rate on the amount adsorbed. Similar results were obtained for the series of samples activated at 800 °C. The apparent rate constants that led to the best-fit of the experimental uptake curves are shown in Table 4. Note that the apparent adsorption rate constants of PPSCT105A7 are one order of magnitude lower than those of PPSA7, PPSCT101A7 and PPSCT102A7. This is probably due to a greater diffusional resistance in the less developed porosity of PPSCT105A7.

Table 4. Apparent rate constants for the adsorption of CO_2 on the activated pellets

	Pseudo-first order model: LDF		Pseudo-second order model: QDF	
Sample	k (s^{-1})	Goodness of fit[a]	k (s^{-1})	Goodness of fit[a]
PPSA7	0.044	2	0.075	12
PPSCT101A7	0.041	1	0.081	6
PPSCT102A7	0.031	2	0.068	5
PPSCT105A7	0.003	5	0.008	2
PPSCT105A8	0.004	8	0.008	2
PPSCT105OxA8	0.017	3	0.029	3

[a] Defined by Equation 10

3.4. Effect of air-oxidation pretreatment

Prior to subjecting the composite pellets to oxidation treatment with air, the reactivity of the individual components in air was assessed in the thermogravimetric analyzer (the results can be found in the supporting information). When CT is heated in a mixture of N_2 and CO_2, mass loss occurs in a single stage. However, when CT is heated in an air flow, two clearly differentiated temperature ranges of mass loss can be appreciated: the first can be attributed to the devolatilization of the coal tar pitch (this is slightly shifted to lower temperatures probably due to the combustion of the volatiles released), and the second is attributed to the combustion of the remaining solid which starts at approximately 500 °C and is nearly complete at 680 °C. The combustion rate of CT reaches its maximum value at around 550 °C. It is particularly worth noting that the mass loss profiles intersect twice: at 360 °C and at 580 °C. Between those temperatures, CT experiences a greater mass loss in the mixture of CO_2 and N_2

than in air. This is attributed to the polymerization of the light components of the coal tar pitch to form cross-linked molecules in the presence of air [29]. When PS is heated in air, two mass loss zones that partially overlap each other are observed. The first starts at about 200 °C and is due to devolatilization of the biomass. As in the case of CT, this is slightly shifted to lower temperatures (the maximum rate of mass loss occurring at 315 °C). The second stage is due to the combustion of the remaining char, which is nearly complete at 490 °C.

To assess the effect of air oxidation pretreatment on the properties of the carbons developed from pine sawdust and coal tar pitch blends, PPSCT105 was subjected to oxidation with air and then activated with CO_2. The oxidation treatment was carried out in 50 cm^3 min^{-1} of air flow at a heating rate of 5 °C min^{-1} up to 275 °C, which was held for different oxidation times: 1, 2, 4 and 6 h. The evolution of the carbon yield with the duration of the oxidation treatment is shown in Figure 4. It can be seen that the oxidation yield decreases as the treatment proceeds, with the highest reduction occurring during the first hour, mainly due to the loss of volatile matter. It is worth noting that the mass loss during the oxidation treatment (between 27 and 38 %) is not accompanied by shrinkage of the pellet. At relatively short oxidation times (1-2 h) there is even a slight increase in the pellet volume (+3 %) followed by a moderate reduction in volume as the oxidation time increases (up to 13 % after 6 h).

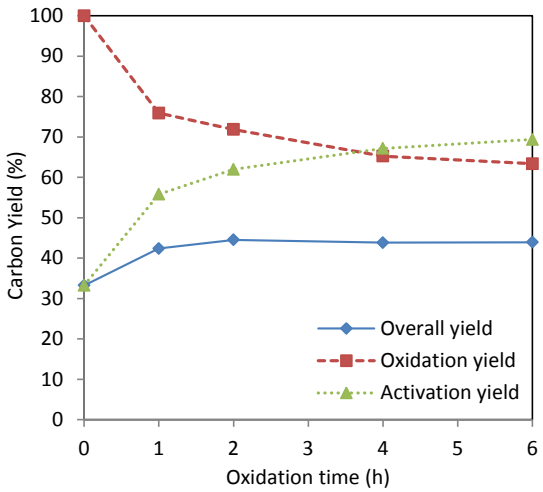

Figure 4. Effect of the duration of the oxidation pretreatment carried out at 275 °C on the carbon yield of PPSCT105.

The oxidized pellets were activated with CO_2 at 800 °C for 30 min, following the same procedure as described for the non-oxidized pellet (PPSCT105A8). The carbon yield of the overall process (oxidation + activation) was significantly higher than the activation yield of PPSCT105 (control sample: oxidation time = 0 h in Figure 4). The greatest shift was observed

for an oxidation time of 1 h (+23%). However, increasing the oxidation time above 2 h had no significant effect on the overall carbon yield, as can be seen in Figure 4.

The PPSCT105 pellets activated after the oxidation pretreatment (PPSCT105OxA8 series) have a similar density to the pellet directly activated with CO_2 (PPSCT105A8): the higher carbon yield of the dual stage process (oxidation + activation) is compensated for by a lower reduction in the volume of the pellets (34 *vs.* 53%).

Figure 5a compares the results from the adsorption tests carried out with the preoxidised-activated-pellets (oxidation times between 1 and 6 h) and the pellet activated without the oxidation pretreatment (0 h). Adsorption tests were conducted under similar conditions to those of the non-oxidized samples. The preoxidised pellets present both higher adsorption capacities and higher adsorption and desorption rates than the control sample. Therefore, the oxidation pretreatment had a positive effect not only on the overall carbon yield of the process, but also on the adsorption performance of the final carbon composites. Increasing the duration of the oxidation treatment beyond 1 h entails no significant benefit from the point of view of adsorption performance. Therefore 1 h was selected as the optimal oxidation soaking time for further study.

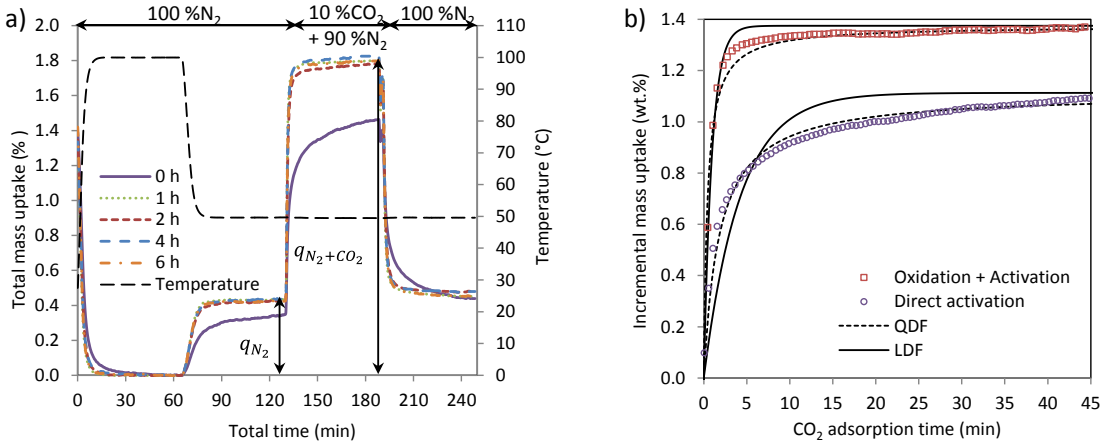

Figure 5. Effect of the oxidation of PPSCT105 on the adsorption performance of the PPSCT105OxA series: (a) total mass uptake *versus* time (full experiment) and (b) incremental mass uptake when the feed gas is changed from 100% N_2 to a mixture containing 90% N_2 and 10% CO_2 at 50 °C.

Figure 5b compares the incremental mass uptake of PPSCT105A8, directly activated with CO_2, with that of the pellet of PPSCT105 activated after oxidation at 275 °C for 1 h (PPSCT105OxA8) when the composition of the feed gas is changed from 100% N_2 to a mixture consisting of 10% CO_2 (balance N_2) at 50 °C. As in the case of PPSCT105A7, the QDF model seems more appropriate for describing the uptake curve of PPSCT105A8 than the LDF approximation (see goodness of fit in Figure 5b and Table 4). In contrast, the uptake curve of PPSCT105OxA8

reflects an intermediate behavior between the LDF and the QDF models. The apparent rate constant that leads to the best fit of the experimental data of PPSCT105A8, as shown in Table 4, is one order of magnitude lower than that of PPSCT105OxA8, which suggests that the oxidation pretreatment has reduced the mass transfer resistance, probably due to a greater development of the pore volume during the subsequent activation stage.

The effect of the temperature of the oxidation pretreatment was also assessed by oxidizing PPSCT105 at different temperatures: 275, 300 and 325 °C for 1 h, and subsequently activating the samples at 800 °C for 30 min. Figure 6 summarizes the overall carbon yield and the total adsorption capacity of these oxidized-activated pellets. When the temperature of the oxidation pretreatment is increased to 300 °C, the overall carbon yield also increases. However, a further increase in the temperature of the oxidation pretreatment up to 325 °C decreases the overall carbon yield of the process significantly. The highest adsorption capacity is attained by the activated pellet preoxidized at 325 °C. A compromise between maximum overall yield and best adsorption performance must be sought, as these two variables have been taken as the decision parameters. Considering that the reduction in carbon yield achieved by increasing the oxidation temperature from 300 to 325 °C was relatively greater than the increase in adsorption capacity, the oxidation temperature of 300 °C was selected to for this study.

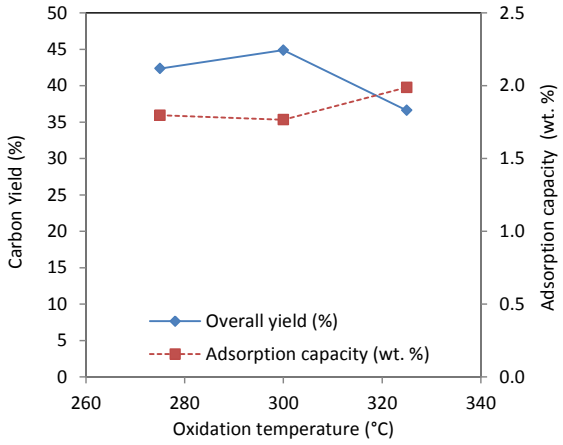

Figure 6. Effect of the temperature of the oxidation pretreatment of PPSCT105 on the overall yield and the adsorption capacity in a mixture consisting of 10 % CO_2 (balance N_2) at atmospheric pressure and at 50 °C

The effect of the activation temperature was reevaluated starting from pellets of PPSCT105 oxidized at 300 °C for 1 h. Figure 7 compares the carbon yield and the adsorption capacity of three samples activated for 30 min at 800, 825 and 850 °C. The adsorption capacity increases with the temperature of activation up to 850 °C. However, the increase in the activation

temperature up to 850 °C also leads to a reduction in the carbon yield due to the increase in the CO_2 gasification rate.

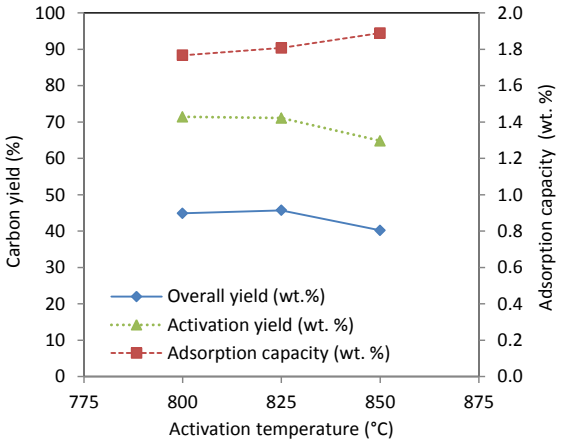

Figure 7. Effect of the temperature of activation on the overall yield and the adsorption capacity in a mixture consisting of 10% CO_2 (balance N_2) at atmospheric pressure and at 50 °C of PPSCT105 oxidized at 300 °C for 1h.

The effect of the time of activation was then assessed at 800 °C using the pellets of PPSCT105 oxidized at 300 °C for 1 h. Figure 8 shows the overall carbon yield and the adsorption capacity of three samples activated for 0.5, 1 and 2 h. As expected, an increase in the activation time reduces the carbon yield due to a greater consumption of carbon atoms by the gasification reaction with CO_2, which develops the pore volume of the pellet, thereby increasing its adsorption capacity.

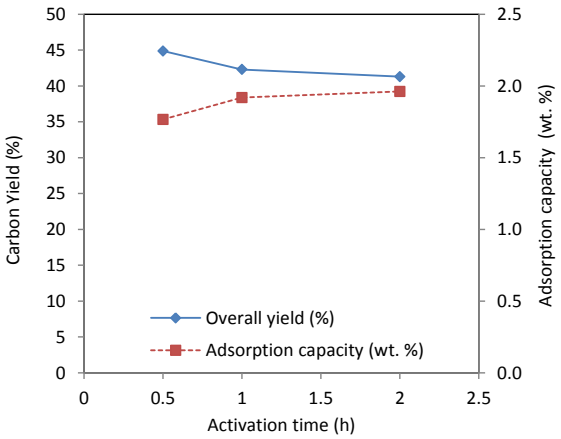

Figure 8. Effect of the activation time at 800 °C on the overall yield and the adsorption capacity in a mixture consisting of 10% CO_2 (balance N_2) at atmospheric pressure and at 50 °C of PPSCT105 oxidized at 300 °C for 1h.

For an activation time of 2 h at a temperature of 800 °C and using pellets of a blend of pine sawdust and coal tar pitch in a mass ratio of 10:5 (PPSCT105) preoxidized in air at 300 °C for 1 h, an impressive overall carbon yield (41 wt.%) was obtained. This sample shows a high

adsorption capacity (2 wt. %) in a mixture with 10% CO_2 (balance N_2) at atmospheric pressure and at 50 °C (which is slightly above that of the reference carbon Norit R2030 CO2) and fast adsorption kinetics. These conditions were considered optimal.

3.5. Adsorbent preparation and characterization

A greater amount of adsorbent was prepared from PPSCT105 in the conditions identified as optimal (oxidation at 300 °C for 1h + activation with CO_2 at 800 °C for 2 h) using a quartz reactor in a vertical furnace. This sample will be referred to as IH2 hereafter. The carbon yield of IH2 was 40%, in good agreement with the results obtained in the thermogravimetric analyzer. It is worth noting that this is an extraordinarily high yield for a wood-based carbon adsorbent: the typical carbon yield for physical and chemical activation are 12.5 and 22%, respectively [24]. Some of the volatiles solidified on the reactor wall (7%), but no liquid tars were collected in the ice bath. The gas yield, calculated by difference, was 53%.

A second sample was prepared from PPS by activation with CO_2 at 800 °C for 1 h. This sample will be referred to as IH3 hereafter. The carbon yield of IH3, 17%, is substantially lower than that of IH2 despite the shorter activation time used, in good agreement with the trends observed in the thermogravimetric analyzer. As in the case of IH2, some of the volatiles solidified on the reactor wall (9%). However, in the case of IH3, a significant amount of liquid tars was collected in the ice batch (35%). The gas fraction, calculated by difference, was lower than that observed for IH2 (39%).

The mechanical resistance of IH2 and IH3 was compared by subjecting these samples to the rotary test described in the experimental section. The hardness number of IH2 (93%) nearly doubles that of IH3 (46%), which is in good agreement with the observations by visual inspection during the handling of the samples.

The lack of a liquid fraction in the case of IH2 in opposition to the relatively high liquid fraction of IH3 was initially attributed to the combustion of the volatiles during the oxidation step. To confirm this hypothesis, a third sample (IH4) was prepared by direct activation of PPSCT105 following the same protocol as for IH2 except for the absence of the pre-oxidation treatment. Nevertheless, no liquid tars were collected in the ice bath during the preparation of IH4, despite the lack of the oxidation stage, which rules out the initial hypothesis of the combustion of the volatiles. It therefore seems likely that the non-production of a liquid fraction is related to the interaction between the pine and the coal tar pitch during the heating process: the tars released from the pine sawdust during heating apparently react with the coal tar pitch, increasing the carbon yield of the blend. Nonetheless, by the end of the activation stage, the

solid fraction of IH4 was merely a cluster of aggregated pellets and only a few isolated pellets could be recovered for characterization purposes. The gas fraction obtained during the preparation of IH4 was 52%, which is similar to that of IH2.

Figure 9 compares the SEM images of the exterior and the interior of the pellets of IH2, IH3 and IH4. The outer morphology of IH2 shows large macropores that must have been formed in the interstitial spaces between the pine sawdust and the coal tar pitch granules. These large pores can act as transport pores, facilitating the diffusion of adsorbates into the pellet. However, adsorption does not take place in these large pores but in the micropores (< 2 nm) which are not visible at these augmentations. It is worth noting that the dimensions of IH2 are close to those of the green pellet before the oxidation and activation treatments (see PPSCT105 in Table 2). IH3 has a significant lower pellet size and a denser structure than IH2. The granules of sawdust are easily appreciated in the interior of IH3: they have a structure that clearly reflects its woody origin. On the other hand, the interior of a pellet of IH2 shows a more continuous phase, formed by a mixture of fibers (arising from pine sawdust) and sponge-like structures (coming from the coal tar pitch). Note that the pellet dimensions of IH4 are closer to those of IH3 than to those of IH2. As mentioned before, the pre-oxidation treatment inhibits the shrinkage of the composite pellet. The absence of oxidation treatment can also be appreciated in the interior of IH4: the matrix of the coal tar pitch has a denser appearance compared to the sponge-like appearance of IH2.

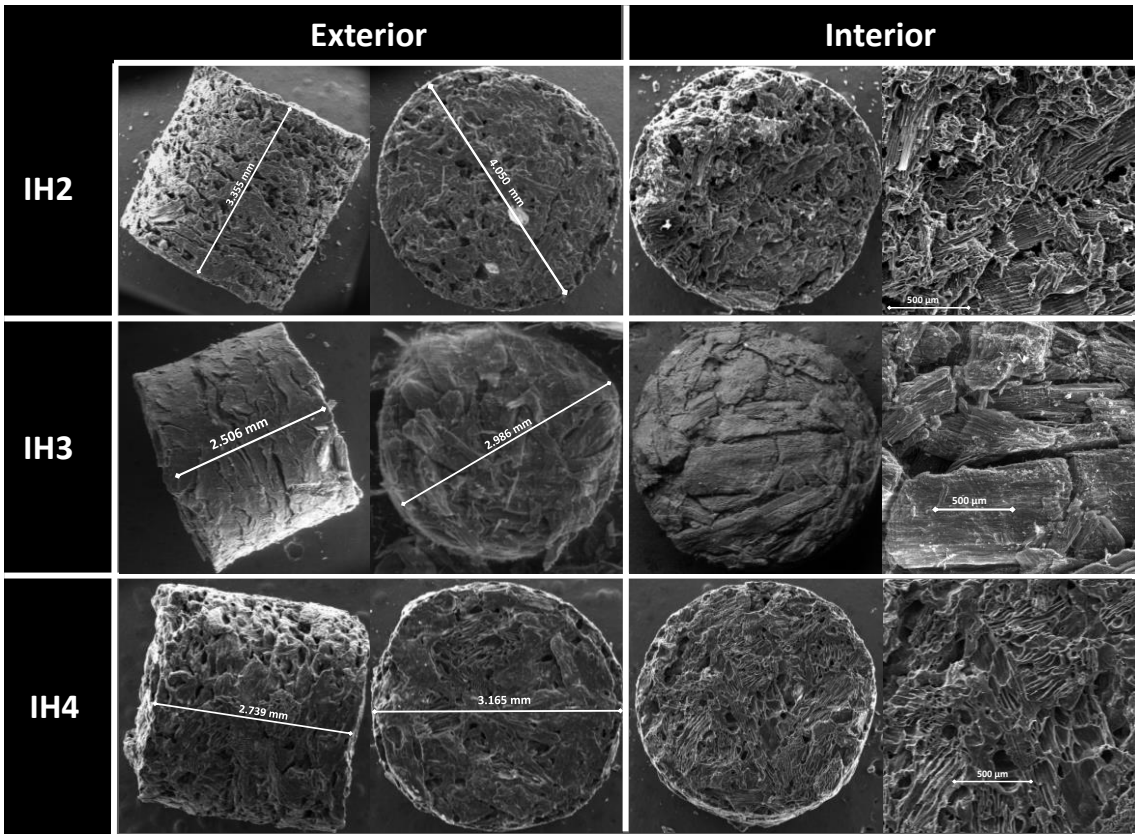

Figure 9. SEM micrographs of samples IH2, IH3 and IH4.

The IH2, IH3 and IH4 pellets were characterized by means of N_2 adsorption at -196 °C. The textural parameters are summarized in Table 5. As can be seen, the samples are essentially microporous. The pine-derived carbon, IH3, presents a higher micropore volume than IH2 and a slightly wider average micropore width. The composite pine-pitch pellets (IH2) have the largest share of micropore volume, which amount to 94% of the total pore volume, and the lowest micropore width: 0.57 nm. IH4 shows the least textural development, confirming the importance of the oxidation pretreatment in the preparation of carbon adsorbents from blends of pine sawdust and coal tar pitch.

Table 5. Textural parameters obtained from the adsorption isotherm of N_2 at -196 °C.

Adsorbent	Precursor	Treatment	S_{BET} ($m^2\ g^{-1}$)	V_p ($cm^3\ g^{-1}$)	V_{DR} ($cm^3\ g^{-1}$)	L_0 (nm)
IH2	PPSCT105	Oxidation (300 °C 1h) + CO_2 activation (800 °C 2h)	561	0.20	0.21	0.57
IH3	PPS	CO_2 activation (800 °C 1h)	783	0.33	0.30	0.75
IH4	PPSCT105	CO_2 activation (800 °C 2h)	281	0.13	0.11	0.74
Norit R2030CO2	Peat	Steam activation (900 °C)	942	0.41	0.39	1.22

The adsorption performance of these samples was evaluated at 50 °C and at atmospheric pressure in the thermogravimetric analyzer and compared to that of the reference carbon Norit R2030CO2. In Figure 10 the adsorption capacities of the samples at equilibrium, both in 100% N_2 and in a mixture consisting of 10 % CO_2 (balance N_2), are compared on a mass basis. The commercial carbon shows the highest N_2 uptake followed by IH3. This is attributed to their higher pore volume. However, the greatest mass uptake from the post-combustion mixture is attained by IH3, which has a lower micropore volume than Norit R2030CO2 but significantly narrower micropore size (see Table 5). Narrow micropores are of the utmost importance for the adsorption of CO_2 in postcombustion conditions (low partial pressures of CO_2) [36-38]. IH2 and IH3 show a slightly lower adsorption capacity than their homologous samples obtained in the thermogravimetric analyzer, but nevertheless the relative trend is maintained.

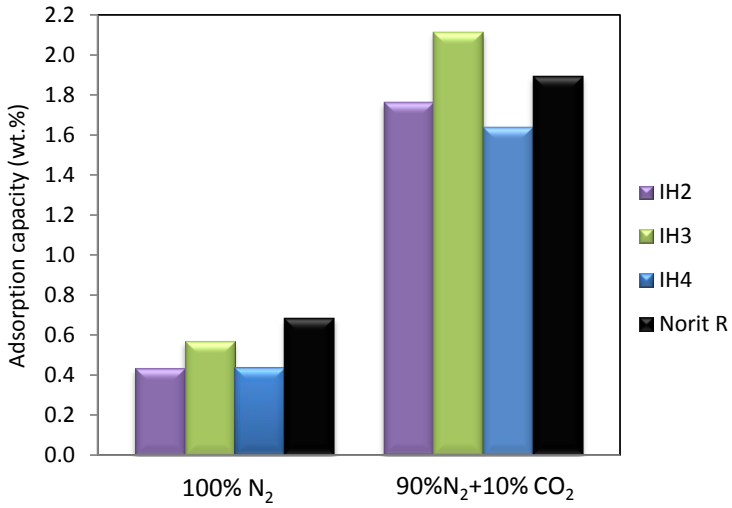

Figure 10. Adsorption capacity expressed on a mass basis of samples IH2, IH3, and carbon Norit R2030CO2 at 50 °C and at atmospheric pressure at equilibrium in 100% N_2 and in a mixture consisting of 10% CO_2 (balance N_2).

Figure 11 compares the dynamic mass uptake of the samples initially saturated with N_2 at 50 °C when a mixture with 10% CO_2 (balance N_2) is fed into the analysis chamber at 50 °C and at atmospheric pressure. The rate of adsorption on IH2, IH3 and Norit R2030CO2 can be adequately described by the LDF model using the following apparent adsorption rate constants: 0.026 s^{-1} for IH2, 0.046 s^{-1} for IH3 and 0.028 s^{-1} for Norit R2030CO2. The uptake curve of IH4 presents a slower approach to equilibrium capacity that is best matched by the QDF model (apparent rate constant: 0.042 s^{-1}). The incremental mass uptake at equilibrium, which is an underestimation of the real amount of CO_2 adsorbed, follows the order: IH3 > IH2 > Norit R2030CO2 ≈ IH4. That is: the adsorbent pellets prepared from pine sawdust (IH3) and from an oxidized blend of pine sawdust and coal tar pitch (IH2) show a CO_2

adsorption capacity, in conditions representative of postcombustion capture, higher than that of the reference carbon, and also fast adsorption kinetics, which make these materials highly appealing adsorbents for post-combustion CO_2 capture.

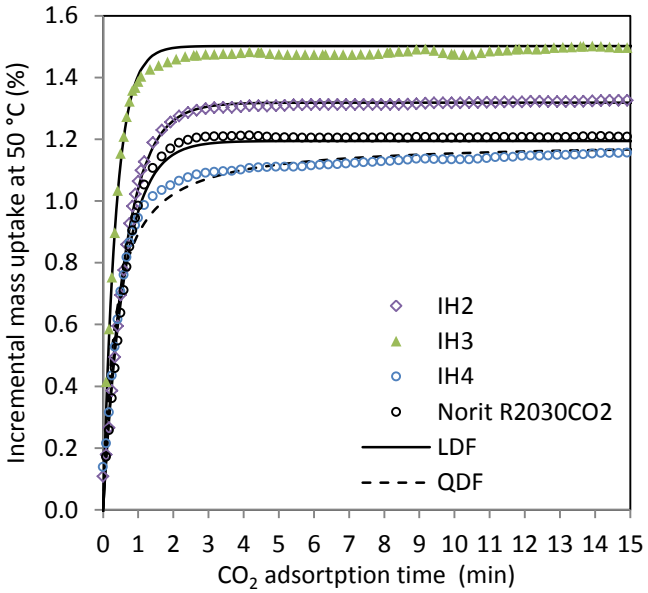

Figure 11. Dynamic mass uptake of samples IH2, IH3, IH4 and Norit R2030CO2 when the composition of the feed gas is changed from 100% N_2 to a mixture consisting of 90% N_2 and 10% CO_2 at 50 °C and at atmospheric pressure.

Conclusions

The adsorbent pellets produced from blends of pine sawdust and coal tar pitch by direct activation with CO_2 show remarkably high carbon yields of up to 35%, which is greater than might be expected from the additive rule. The oxidation of the composite pellets with air prior to their activation with CO_2 led to a further improvement in the carbon yield of the overall process, reaching values of up to 45%. This is an extraordinarily high carbon yield for a wood-based activated carbon, which usually provides total carbon yields of between 12 and 22%. Therefore these composites present an attractive economic incentive for its production on a industrial scale.

The oxidation pretreatment also had a promoting effect on the CO_2 adsorption capacity and kinetics of the final adsorbents.

Another important advantage of the pine-pitch adsorbent pellets for their application in cyclic adsorption processes is their superior mechanical resistance: their hardness number (96%) nearly doubles that of the adsorbent pellets produced from pine sawdust alone (46%).

Acknowledgements

This work was carried out with financial support from the Spanish MINECO (Project ENE2011-23467), co-financed by the European Regional Development Fund (ERDF). M.G.P. acknowledges funding from the CSIC (JAE-Doc program), co-financed by the European Social Fund, and I.D. acknowledges funding from the Government of the Principado de Asturias.

The authors are grateful to Industrial Química del Nalón S.A. for supplying the coal tar pitch sample.

References

[1] O. Ioannidou, A. Zabaniotou, Agricultural residues as precursors for activated carbon production - A review. *Renew Sustainable Energy Rev*, **11** (2007), pp.1966-2005.

[2] A.R. Mohamed, M. Mohammadi, G.N. Darzi, Preparation of carbon molecular sieve from lignocellulosic biomass: A review. *Renew Sustainable Energy Rev*, **14** (2010), pp.1591-1599.

[3] M.G. Plaza, C. Pevida, B. Arias, M.D. Casal, C.F. Martín, J. Fermoso*, et al.*, Different approaches for the development of low-cost CO_2 adsorbents. *J Environ Eng-ASCE*, **135** (2009), pp.426-432.

[4] M.G. Plaza, C. Pevida, B. Arias, J. Fermoso, M.D. Casal, C.F. Martín*, et al.*, Development of low-cost biomass-based adsorbents for postcombustion CO_2 capture. *Fuel*, **88** (2009), pp.2442-2447.

[5] M.G. Plaza, C. Pevida, C.F. Martín, J. Fermoso, J.J. Pis, F. Rubiera, Developing almond shell-derived activated carbons as CO_2 adsorbents. *Sep Purif Technol*, **71** (2010), pp.102-106.

[6] M.G. Plaza, F. Rubiera, J.J. Pis, C. Pevida, Ammoxidation of carbon materials for CO_2 capture. *Appl Surf Sci*, **256** (2010), pp.6843-6849.

[7] M.G. Plaza, S. García, F. Rubiera, J.J. Pis, C. Pevida, Evaluation of ammonia modified and conventionally activated biomass based carbons as CO_2 adsorbents in postcombustion conditions. *Sep Purif Technol*, **80** (2011), pp.96-104.

[8] M.G. Plaza, A.S. González, C. Pevida, J.J. Pis, F. Rubiera, Valorisation of spent coffee grounds as CO_2 adsorbents for postcombustion capture applications. *Appl Energ*, **99** (2012), pp.272-279.

[9] M.G. Plaza, A.S. González, J.J. Pis, F. Rubiera, C. Pevida, Production of microporous biochars by single-step oxidation: Effect of activation conditions on CO_2 capture. *Appl Energ*, **114** (2014), pp.551-562.

[10] M.G. Plaza, A.S. González, C. Pevida, F. Rubiera, Influence of water vapor on CO_2 adsorption using a biomass-based carbon. *Ind Eng Chem Res*, **53** (2014), pp.15488−15499.

[11] X.-L. Zhu, P.-Y. Wang, C. Peng, J. Yang, X.-B. Yan, Activated carbon produced from paulownia sawdust for high-performance CO2 sorbents. *Chinese Chemical Letters*, **25** (2014), pp.929-932.

[12] W. Hao, E. Björkman, M. Lilliestråle, N. Hedin, Activated carbons prepared from hydrothermally carbonized waste biomass used as adsorbents for CO_2. *Appl Energ*, **112** (2013), pp.526-532.

[13] M. Olivares-Marín, M.M. Maroto-Valer, Development of adsorbents for CO_2 capture from waste materials: a review. *Greenhouse Gases: Science and Technology*, **2** (2012), pp.20-35.

[14] B. Huang, S. Xu, S. Gao, L. Liu, J. Tao, H. Niu*, et al.*, Industrial test and techno-economic analysis of CO_2 capture in Huaneng Beijing coal-fired power station. *Appl Energ*, **87** (2010), pp.3347-3354.

[15] K. Goto, K. Yogo, T. Higashii, A review of efficiency penalty in a coal-fired power plant with post-combustion CO2 capture. *Appl Energ*, **111** (2013), pp.710-720.

[16] M.T. Ho, G.W. Allinson, D.E. Wiley, Reducing the cost of CO_2 capture from flue gases using pressure swing adsorption. *Ind Eng Chem Res*, **47** (2008), pp.4883-4890.

[17] M. Radosz, X. Hu, K. Krutkramelis, Y. Shen, Flue-gas carbon capture on carbonaceous sorbents: toward a low-cost multifunctional carbon filter for "green" energy producers. *Ind Eng Chem Res*, **47** (2008), pp.3783-3794.

[18] J. Zhang, P.A. Webley, P. Xiao, Effect of process parameters on power requirements of vacuum swing adsorption technology for CO_2 capture from flue gas. *Energ Convers Manage*, **49** (2008), pp.346-356.

[19] N. Hedin, L. Chen, A. Laaksonen, Sorbents for CO_2 capture from flue gas-aspects from materials and theoretical chemistry. *Nanoscale*, (2010).

[20] M.J. Antal, M. Grønli, The Art, Science, and Technology of Charcoal Production†. *Ind Eng Chem Res*, **42** (2003), pp.1619-1640.

[21] R. Pietrzak, Sawdust pellets from coniferous species as adsorbents for NO2 removal. *Bioresour Technol*, **101** (2010), pp.907-913.

[22] P. Nowicki, R. Pietrzak, Carbonaceous adsorbents prepared by physical activation of pine sawdust and their application for removal of NO2 in dry and wet conditions. *Bioresour Technol*, **101** (2010), pp.5802-5807.

[23] A. Heidari, H. Younesi, A. Rashidi, A.A. Ghoreyshi, Evaluation of CO2 adsorption with eucalyptus wood based activated carbon modified by ammonia solution through heat treatment. *Chem Eng J*, **254** (2014), pp.503-513.

[24] G.G. Stavropoulos, A.A. Zabaniotou, Minimizing activated carbons production cost. *Fuel Process Technol*, **90** (2009), pp.952-957.

[25] B. Pendyal, M.M. Johns, W.E. Marshall, M. Ahmedna, R.M. Rao, The effect of binders and agricultural by-products on physical and chemical properties of granular activated carbons. *Bioresour Technol*, **68** (1999), pp.247-254.

[26] C. Ng, W. Marshall, R.M. Rao, R.R. Bansode, J.N. Losso, R.J. Portier. Granular activated carbons from agricultural by-products: process description and estimated cost of production. Baton Rouge, LA: LSU Agricultural center; 2003.

[27] J. Alcañiz-Monge, J.P. Marco-Lozar, D. Lozano-Castelló, Monolithic Carbon Molecular Sieves from activated bituminous coal impregnated with a slurry of coal tar pitch. *Fuel Process Technol*, **95** (2012), pp.67-72.

[28] T. Wigmans, Industrial aspects of production and use of activated carbons. *Carbon*, **27** (1989), pp.13-22.

[29] C. Blanco, R. Santamaría, J. Bermejo, R. Menéndez, A comparative study of air-blown and thermally treated coal-tar pitches. *Carbon*, **38** (2000), pp.517-523.

[30] S. Loganathan, M. Tikmani, S. Edubilli, A. Mishra, A.K. Ghoshal, CO2 adsorption kinetics on mesoporous silica under wide range of pressure and temperature. *Chem Eng J*, **256** (2014), pp.1-8.

[31] F. Stoeckli, L. Ballerini, Evolution of microporosity during activation of carbon. *Fuel*, **70** (1991), pp.557-559.

[32] M.V. Gil, P. Oulego, M.D. Casal, C. Pevida, J.J. Pis, F. Rubiera, Mechanical durability and combustion characteristics of pellets from biomass blends. *Bioresour Technol*, **101** (2010), pp.8859-8867.

[33] Calgon. Defining pore properties. Information Bulletin: Calgon carbon Corporation; IB-1033-06/93.

[34] CEFIC. Tests methods for Activated carbon: European Council of Chemical Manfacturers' Federation; 1986.

[35] P. Álvarez, C. Blanco, R. Santamaría, M. Granda, Lignocellulose/pitch based composites. *Composites Part A: Applied Science and Manufacturing*, **36** (2005), pp.649-657.

[36] M.G. Plaza, C. Pevida, A. Arenillas, F. Rubiera, J.J. Pis, CO_2 capture by adsorption with nitrogen enriched carbons. *Fuel*, **86** (2007), pp.2204-2212.

[37] C.F. Martín, M.G. Plaza, J.J. Pis, F. Rubiera, C. Pevida, T.A. Centeno, On the limits of CO_2 capture capacity of carbons. *Sep Purif Technol*, **74** (2010), pp.225-229.

[38] V. Presser, J. McDonough, S.-H. Yeon, Y. Gogotsi, Effect of pore size on carbon dioxide sorption by carbide derived carbon. *Energ Environ Sci*, **4** (2011), pp.3059-3066.